Dynamics of accretion columns in X-ray pulsars: shocks, pulsations, and subsonic regime

Pavel Abolmasov[1,2] Galina Lipunova[3]

[1]University of Tel Aviv [2] SCEECS [3]MPIfR Bonn

Motivation and simulation setup

- motion inside the magnetosphere of a strongly magnetized NS is essentially force-free, but along the field line may be treated in terms of one-dimensional hydrodynamics (bead-on-a-wire approximation)
- the flow is subsonic at the outer edge and ends subsonic near the surface
- depending on the parameters, the flow may be transonic (with a shock wave near the surface or an elevated *accretion column*)
- steady-state global structure of an accretion column was considered by Basko & Sunyaev (1976)
- time-dependent structure of an accretion column in NSs was considered in Abolmasov & Lipunova (2023), see bottom figure
- existence of a subsonic magnetospheric flow was never considered (?)

Fiducial model:

- $\dot{M} = \dot{m} L_{\rm Edd}/c^2 = 10 L_{\rm Edd}/c^2$ ($L_{\rm Edd}$ is Eddington luminosity)
- $\mu = 10^{29}{\rm G\,cm^3}$ (surface field $\sim 10^{11}{\rm G}$)
- magnetosphere size $R_{\rm e} \sim 14 R_*$
- $\Delta R_{\rm e}/R_{\rm e} = 1/4$, azimuthal size restricted to $\Delta\varphi = 2\pi a = \pi/2$
- cells where $P \geq P_{\rm mag}$ lose mass, energy, and momentum

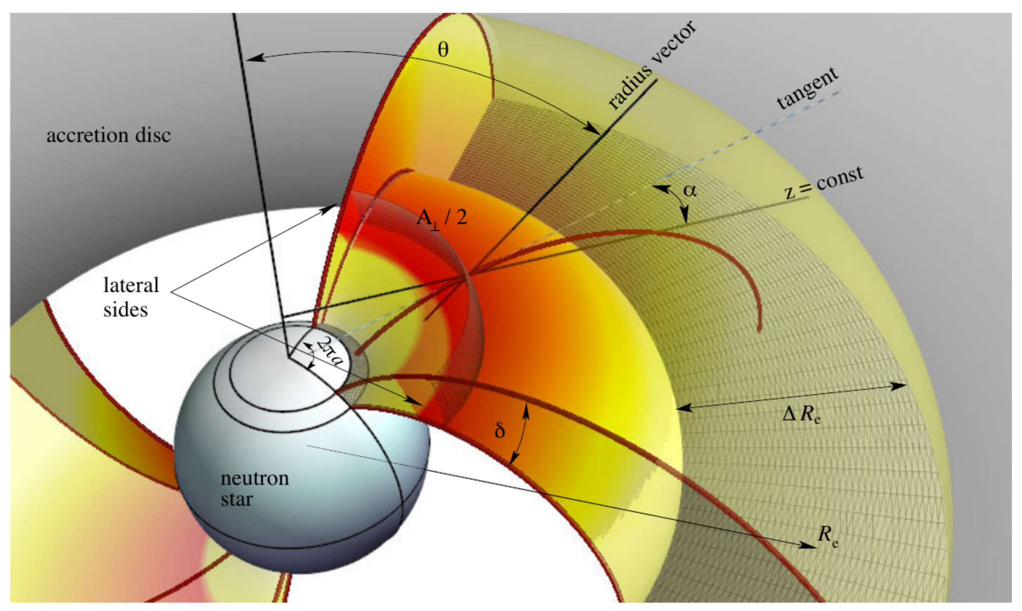

Figure 1. Sketch illustrating geometry of the magnetospheric flow.

Comparison to the analytic solution

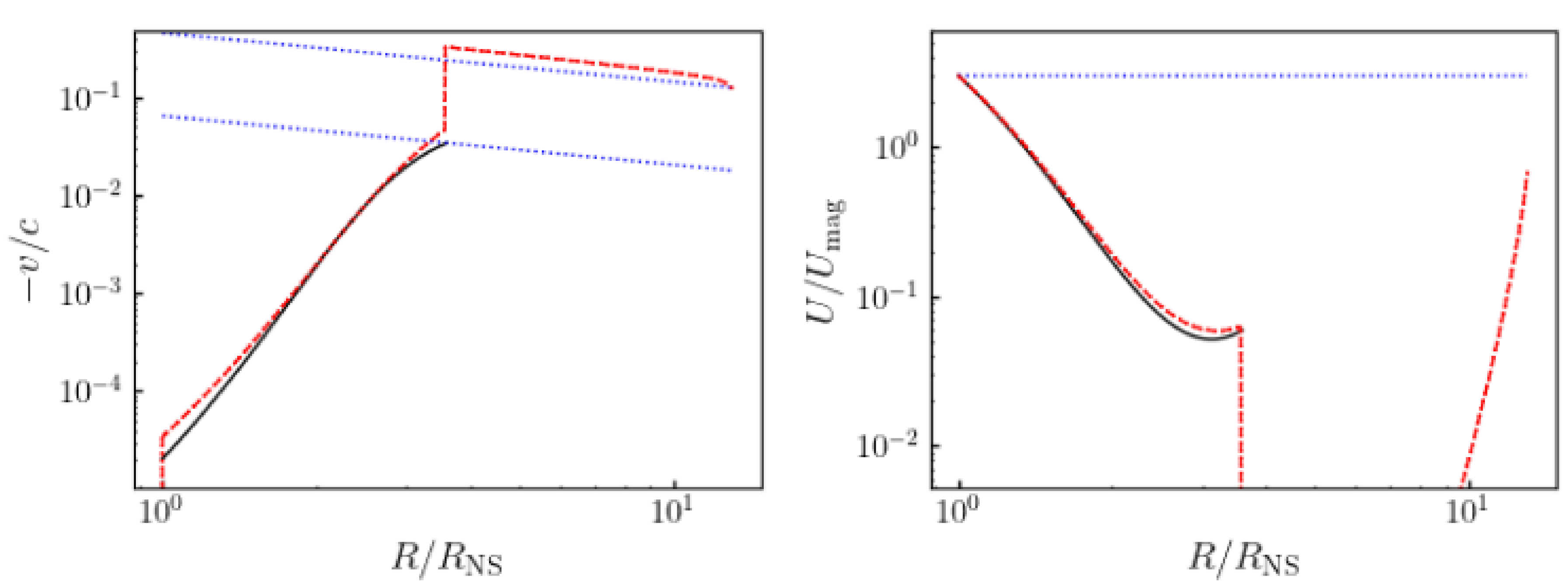

Figure 2. Energy density (compared to magnetic field energy density) and velocity inside the accretion column. Analytic model (Basko & Sunyaev 1976) is shown by solid black lines, red lines are time-averaged values from the simulation

Presence of the shock

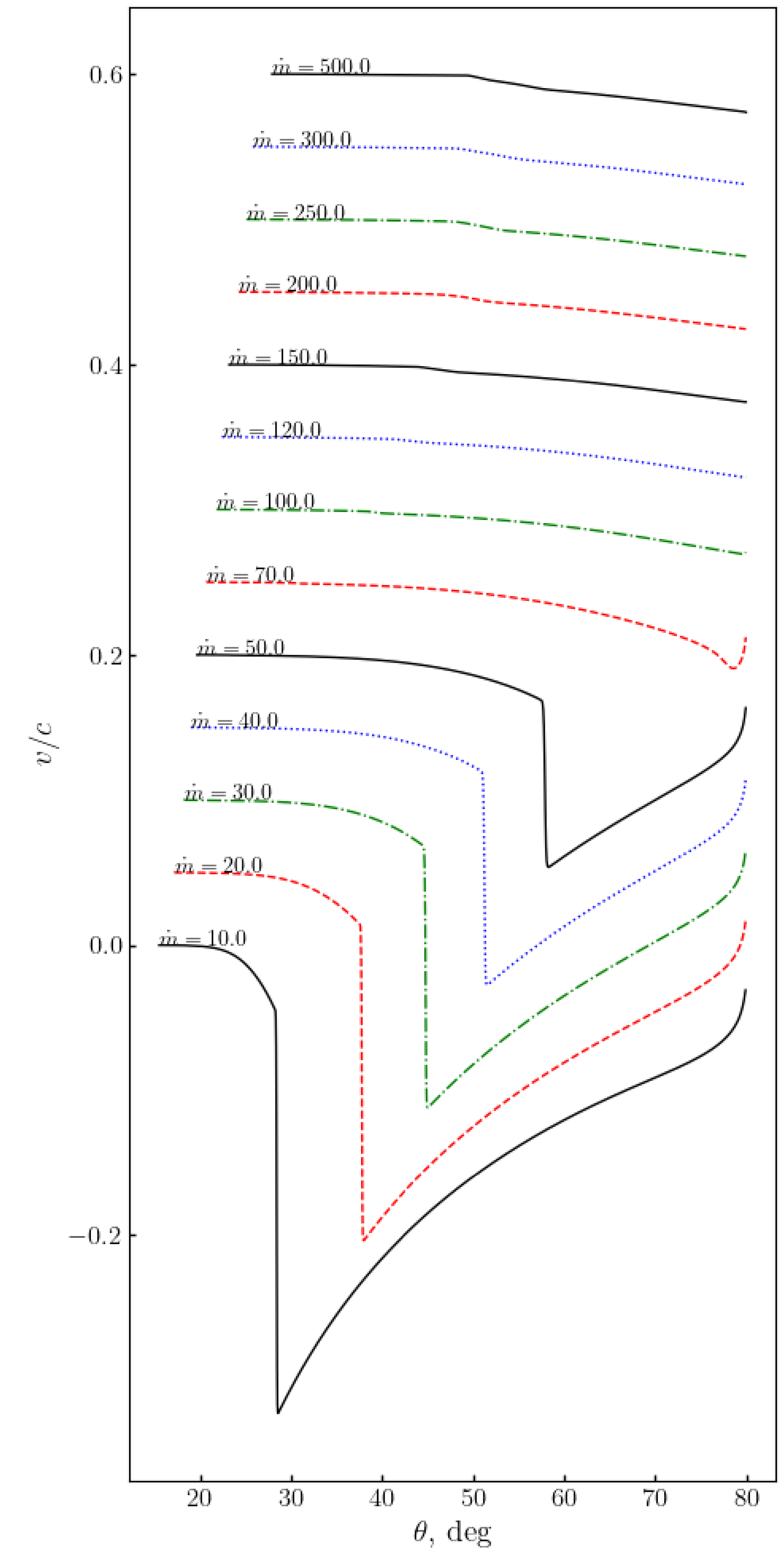

Figure 3. Velocity as a function of polar angle for different mass accretion rates. Each successive curve is shifted in vertical direction by 0.05. Results of a series of simulations with $\mu = 10^{29}{\rm G\,cm^3}$, $a = 0.25$, and $\Delta R_{\rm e}/R_{\rm e} = 0.25$. The shock wave may be traced for the lower mass accretion rates up to $\dot m = 50$, and then disappears.

Subsonic flow

The two basic equations are Euler (hydrostatic)

$$\frac{1}{\rho}\frac{{\rm d}P}{{\rm d}\theta} = -\frac{2GM_*}{R_{\rm e}}\frac{\cos\theta}{\sin^3\theta}, \qquad (1)$$

and energy

$$e^{-k\cos\theta(1+\cos^2\theta)}\frac{\rm d}{{\rm d}\theta}\left[e^{k\cos\theta(1+\cos^2\theta)}\frac{u}{\rho}\right] = -\frac{3\cos\theta}{2\sin^3\theta}\frac{GM}{R_{\rm e}}, \qquad (2)$$

equations. Here, θ is polar angle, $R_{\rm e}$ is magnetospheric radius, and

$$k = \frac{aR_{\rm e}}{\Delta R_{\rm e}}\frac{R_{\rm e}c^2}{GM}\frac{1}{\dot m} \sim \frac{R_{\rm e}}{R_{\rm sph}}. \qquad (3)$$

measures the radiative cooling of the column (low k is advective).

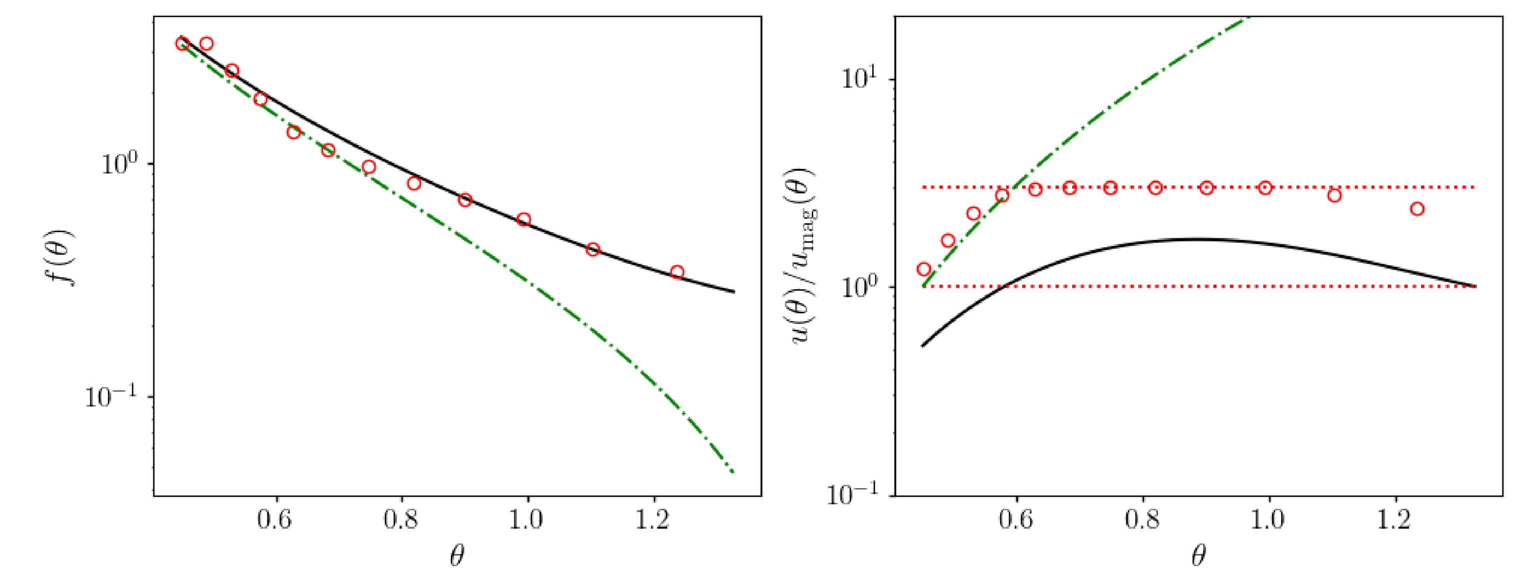

Figure 4. Normalized enthalpy $f = \dfrac{u}{\rho}\dfrac{R_{\rm e}}{GM}$ (left panel) and energy density u in the magnetic energy density units (right panel). Semi-analytical subsonic solution produced by numerical integration of Eqs. (1) and (2) is shown by the solid black lines. Red circles show time-averaged numerical solution, low-k analytic solution is shown by green dot-dashed lines.

Development of a subsonic flow

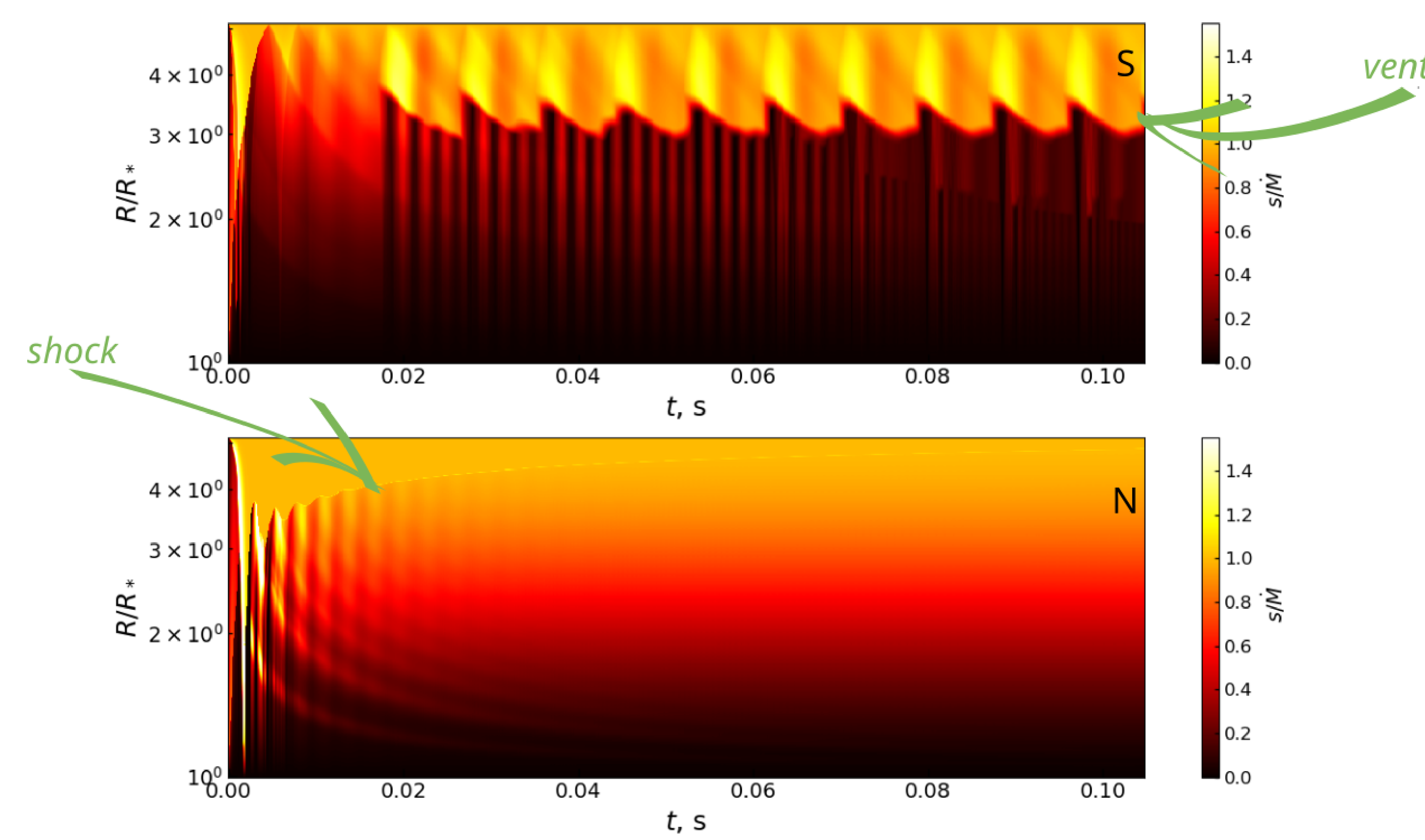

Figure 5. Local mass accretion rate $s = \rho v A_\perp$ plotted as a function of radius and time for two $\dot m = 300$ models, with (upper) and without (lower) mass loss allowed.

Time-radius diagram for shock oscillations

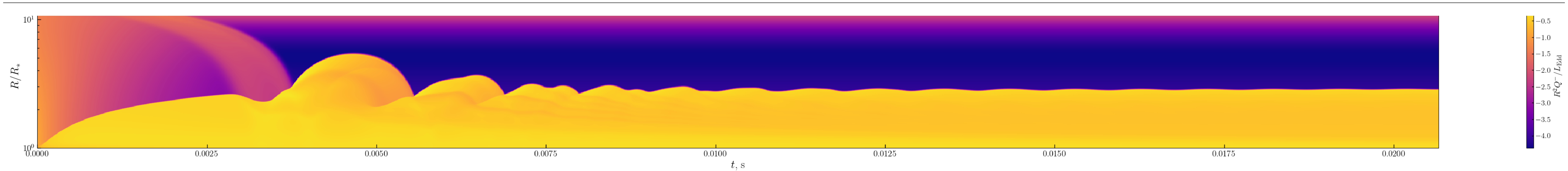

Figure 6. Normalized radiation flux from the surface of the magnetospheric flow, shown as a function of time (seconds) and radius (NS radius units). The shock front stabilises at about $3.6R_*$.